Journal of Animal Environment

(E-ISSN 2717-1396, ISSN 2717-1388)

Original Research Paper

Ecofriendly Green Synthesis and Comparative Physicochemical Characterization of Fe–Cu Bimetallic Nanoparticles Using *Caralluma attenuata* Root Extract under Thermal and Non-Thermal Conditions

Konathala Sirisha Rani [1], K Suresh Babu [2*]

[1]Research Scholar, BEST Innovation University, Gownivaripalli, Gorantla, Andhra Pradesh 515231, India.

[1]Asst Professor, St Pious X Degree and PG College for Women, Nacharam, Secunderabad, India.

[2] Department of Chemistry, Marri Laxman Reddy Institute of Technology and Management, Hyderabad, India.

Corresponding author:

Dr K Suresh Babu

E Mail: babuiict@gmail.com, sureshbabuiict1@gmail.com

ABSTRACT

Sustainable bimetallic nanostructures via plant-based systems gained popularity for replacing chemical pathways. In this work, the synthesis of Fe -Cu bimetallic nanoparticles was conducted with *Caralluma attenuata* root extract as a dual functioning reducing and stabilizing agent in thermal and non thermal approach. In this multi spectral characterization were employed to compare the efficiency of the synthesized bimetallic systems. The X-ray diffraction confirmed the formation of an Fe-rich face-centred cubic (fcc) lattice with a minor amount of Cu. The FTIR and Raman spectra showed the presence of bioactive phytochemicals in the reduction, capping and stabilization of metal. UV-visible spectroscopy showed that there were very strong surface plasmon resonances connected to Fe domains and Fe-Cu interaction. Dielectric measurements showed frequency-relaxing permittivity relaxation behaviour, interfacial polarization and charge transport behaviour that varied with precursor volume and thermal treatment. Morphology of the surface of thermal treated sample was good interfacial properties as shown by SEM micrographs. This confirms that *Caralluma* extract triggers a regulated nucleation-growth route, leading to extremely stable hybrid nanostructures with controllable optical and electrical features. These results demonstrate heat processed Fe-Cu bimetallic nanoparticles colud be applicable as catalysts, dielectric and multifunctional nanotechnological agents.

KEYWORDS ***Caralluma attenuata*, Fe-Cu bimetallic nanoparticles, green synthesis, dielectric behaviour, nanocomposites.**

1. Introduction

Nanostructures made of two or more metals have become of great interest due to their desirable physicochemical behaviour. In many applications, such systems have been found to perform better than their monometallic counterparts such as catalysis, electronics, photonics, environmental remediation, and biomedical engineering[1]. Structural architecture (e.g., core-shell, alloyed, heterostructure), composition, particle size, and morphology can be employed to effectively tune the physicochemical properties of bimetallic nanoparticles, directly affecting their surface reactivity, electronic structure, and functional performance, and thus impacting the overall reactivity of bimetallic nanoparticles[2].

Copper (Cu) is a 3d transition metal with physicochemical characteristics like a large electrical and thermal conductivity, catalytic activity, and mechanical strengths[3]. Nevertheless, under ambient conditions, Cu nanoparticles are vulnerable to oxidation, and it can have a significant influence on their stability and functioning.

Iron (Fe) on the other hand is a ferromagnetic substance, which exhibits a high magnetic moment and is highly reductive[4]. Moreover, iron nanoparticles are superparamagnetic, and easily manipulated under external magnetic fields, which is useful in catalyst recovery and targeted catalysts[5]. However, magnetic interaction and high surface energy cause iron nanoparticles to form aggregates, which has low stability and reactivity. The combination of copper and iron into one bimetallic system is a promising approach to eliminating the drawbacks of each of the two metals and bringing their beneficial characteristics together.

Fe-Cu nanostructures are expected to have higher catalytic ability, electron transfer performance, and tenable magnetic behaviour for various

***Corresponding Author:**

Received: 25th May, 2026; Revised: 6th June, 2026; Accepted: 8th June, 2026; Available Online: 3rd July, 2026

(DOI): 10.70102/AEJ.2026.18.2s.48

applications.

Traditional synthesis techniques typically require the use of toxic reagents, lots of energy, and complicated processing environments, which restrict their compatibility with the environment and their scalability. The green synthesis methods based on plant extracts have become sustainable alternatives in the recent years where naturally occurring phytochemicals serve as reducing, capping, and stabilizing agents. The synthesis of metallic and bimetallic nanoparticles by plant-derived systems has been reported in a number of studies[6], [7], [8], but these studies are mainly restricted to characterization of the basic structure and do not show a systematic control of the synthesis parameters. Moreover, the effects of synthesis conditions (including extract concentration and thermal treatment) on the structural development and functional characteristics of bimetallic nanoparticles are not sufficiently discussed in most of the available reports. Specifically, the mechanisms of dielectric behaviour and charge transport in green-synthesized Fe-Cu systems are understudied, although they are crucial in electronic and energy-related studies.

In this regard, *Caralluma attenuata* a phytochemically rich plant that is rich in flavonoids, phenolics, saponins and pregnane glycosides. These bioactive compounds facilitate the effective reduction and stabilization of metal ions and this could result in controlled formation of nanoparticles. Thus, the current research is on the green synthesis of Fe-Cu bimetallic nanoparticles with *Caralluma attenuata* root extract, at which the extraction concentration and heating conditions are varied systematically. A detailed characterization strategy is used to study structural, morphological, optical and dielectric properties, with special focus on creating correlations between the synthesis parameters and functional behaviour. In this study, the researchers want to learn more about the importance of phytochemical-mediated synthesis in the modification of multifunctional nanomaterials and to broaden the scope of application of Fe–Cu nanostructures.

2. Materials

Copper sulfate pentahydrate ($CuSO_4.5H_2O$) and Iron chloride of analysis grade were obtained through certified vendors of Sigma Aldrich, Chennai. The fresh roots of *Caralluma Attenuata* were collected locally which were found in India after being washed, shade dried and cut into minute pieces. Deionized water was used to prepare all the experimental solutions, and no other chemical reducing or stabilizing agents were added, keeping a strictly green synthesis pathway.

2.1 Preparation of *Caralluma Attenuata* Root Extract

About 10g of finely chopped *Caralluma Attenuata* root was boiled in 100ml of deionized water for 30 minutes. After that the mixture was cooled to room temperature and filtered using Whatman filter paper No.1. The filtered filtrate was stored at 4ºc for further analyses. The extract acted simultaneously as a reducing, stabilizing and growth-directing agent due to its high content of phenolics, glycosides and terpenoids.

2.2. Green Synthesis of Cu–Fe Bimetallic Nanostructures

Aqueous solution of ferric chloride and copper sulphate precursors were separately prepared as 0.01M concentration. Then equimolar ration solution of both were mixed together to get homogeneous solution. To the precursor solution the *Caralluma attenuata* extract was added dropwise as 5ml, 10ml, 15ml and 20ml to initiate bio reduction process. At each additions the mixture was stirred and a visible colour change from blue to black indicates the formation of bimetallic Fe-Cu nanoparticles. The mixture obtained was divided into two equal parts and subsequently used for further analysis. The one portion is remained in room temperature and another portion of the mixture was heated from 60-70ºC for 1h. The sample without heat is noted as P and the sample prepared via heating method is noted as T. Both samples were then centrifuged under 8000rpm for 15minutes. Finally, the centrifuged nanoparticles were dried and used for further analysis. Such systematic variation allowed the role of extract concentration and thermal activation in morphology, crystallite structure, optical properties and dielectric response to be comprehended.

2.3 Fourier Transform Infrared Spectroscopy

The Nicolet iS10 spectrometer (Thermo Fisher Scientific, USA) was used to perform Fourier transform infrared (FTIR) spectroscopy to determine the functional groups that are involved in the reduction and stabilization of nanoparticles[9]. A sample of the dried nanoparticles was thoroughly mixed with spectroscopic-grade potassium bromide (KBr) in the ratio of 1:100 and pressed to a pellet using a hydraulic press. The spectrums were measured between 4000 and 400 cm^{-1} at a resolution of 4 cm^{-1} and 32 scans taken of each sample to enhance spectral accuracy.

2.4 UV–Visible Spectroscopy

A UV–visible spectrophotometer (UV-2600, Shimadzu Corporation, Japan) was used to analyse the optical properties and formations of Fe-Cu bimetallic nanoparticles. Absorption spectra were measured in the wavelength of 200-800nm with a spectral resolution of 1nm[10]. Before analysing, the nanoparticle colloidal solution was diluted properly with deionised water to avoid the effects of saturation. About 2 mL of the sample was pipette transferred to a quartz cuvette with a path length of 1 cm and baseline was corrected with the deionized water as a reference. The scan was performed at medium speed so that the accurate peak acquisition can be obtained.

2.4 Raman Spectroscopy

The analysis was conducted by Raman with an inVia Reflex Raman spectrometer (Renishaw plc, UK) with a 532 nm laser source as the exciter. The powdered samples were placed directly to a clean glass substrate with no additional preparation[11]. The spectra were obtained in the region of 100-2000 cm^{-1}. Laser power was kept at low levels to prevent heating of the sample and one spectrum was recorded at a time with acquisition time of 1020 seconds and various accumulations to enhance the quality of the signal.

2.4 X-ray Diffraction (XRD)

X-ray diffractometer (X'Pert PRO, PANalytical B.V., Netherlands) was used to analyze the crystalline structure and purity of the synthesized nanoparticles using the Cu K alpha radiation at a wavelength of 1.5406Å. The finely powdered samples were evenly spread onto the sample holder to obtain a smooth surface[12]. The patterns of diffraction were measured in the range of 20o -80o with step of 0.02^o and scanning rate of 2^o/min. The instrument was run at an accelerating voltage of 40 kV at a current of 30 mA.

2.7 Scanning Electron Microscopy (SEM)

A scanning electron microscope (JSM-7610F, JEOL Ltd., Japan) was used to determine surface morphology and microstructure of the nanoparticles. A sample was placed on a small aluminium stub with a small amount of dried sample using double sided conductive carbon tape. The samples were coated with a thin layer of gold by sputtering, in order to increase its conductivity and reduce the charging effects[13], [14]. The imaging was performed with accelerating voltage of 5-15 kV at various magnifications.

2.8 Dielectric Measurements

Dielectric properties of the Fe-Cu nanoparticles were measured by LCR meter (HIOKI 3532-50 LCR HiTESTER, Hioki E.E. Corporation, Japan). In order to measure them, the nanoparticle powders were pressed to pellets with a diameter of about 10 mm and thickness of about 1-2 mm using hydraulic press[15]. Silver paste was applied on both sides of the pellet to provide good electrical contact. Measurements of the dielectric parameters were conducted at room temperature, in the frequency range (50 Hz) to (5 MHz) and dielectric constant and dielectric loss were measured. The measurements were made with an AC voltage of 1 V, to measure the frequency-dependent electrical behaviour of the samples.

3. Result and Discussion

3.1 FT-IR analysis

As prepared (P) and thermally treated (T) Fe-Cu bimetallic nanoparticles have characteristic vibrational bands in their FTIR spectra as illustrated in Figure 1. The observed absorption bands at 2354 cm^{-1} (P) and 2364 cm^{-1} (T) are usually explained by an asymmetric stretching of the adsorbed CO_2 molecules or carbonate species that are usually left on the nanoparticle surface after exposure to the atmosphere. The small increase in wavenumber in the thermally treated sample indicates the desorption of the weakly bound carbonaceous species and the decrease in surface adsorption sites as a widely documented effect in thermally treated nanomaterials as surface energy minimization creates less contaminated interfaces. The major change in the area of 1733 cm^{-1} and 1745cm^{-1} indicates the C=O of plant phytochemicals as aldehydes, ketones, and esters. These groups are essential in reduction and stabilization of metal ions on the surface of nanoparticles. This blue shift (wavenumber increase) with thermal treatment is a sign of the change of weakly adsorbed organic species into more highly coordinated metal-oxygen bonds, which is an indication of the redistribution of electron density at the metal-ligand interface. In the case of *Ocimum sanctum*-derived Fe nanoparticles, where C=O spectral changes were observed when the nanoparticles were formed, which is an indication of metal-ligand interaction[16]. Similar behaviour was also seen with *Punica granatum* peel-mediated Cu nanoparticles, whereby a blue shift in C=O stretching was observed with changing thermal treatment as a result of a change in weakly adsorbed species to coordinated oxygen donors[17]. The greater change after thermal treatment in the current system would indicate an increased chemisorption and stabilization of Fe–Cu surfaces by using oxygen-containing ligands. Heat treatment favours chemisorption over physisorption in bio-capped nanoparticles, causing the same effects. The bands around 1372-1374 cm^{-1} are attributed to C -H bending vibrations and phenolic O -H deformation. The slight change but low intensity of the bands comparing P and T samples indicates that there was partial degradation or rearrangement of organic capping layers that is in line with thermal degradation of labile phytoconstituents like flavonoids and glycosides. This tendency shows that thermal treatment selectively eliminates loosely bound organic fractions leaving strongly interacting functional groups. The peak absorption at 1218 and 1219 cm^{-1} can be attributed to C -O stretching vibrations of alcohols, ethers and phenolic groups, which are known to be involved in metal ion complexation in the green synthesis. The thermal treatment of the sample results in a sharpening effect and a slight change in the position, which are indicative of a better structure ordering and enhanced anchoring of the oxygen-containing functional groups on the nanoparticle surface. This is an indication of a more stable metalorganic interface formed following thermal activation.

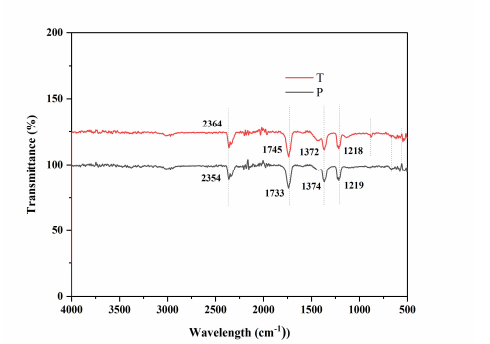

Figure 1 FTIR analysis of as prepared and heat treated Fe-Cu bimetallic nanoparticles

3.2 UV analysis

As prepared (P) and thermally treated (T) Fe-Cu bimetallic nanoparticles have broad, featureless absorption indicated by the UV-visible absorption spectra in Figure 2. The prepared sample has a higher absorbance than the thermally treated sample, suggesting a higher optical density as a result of the presence of surface-bound phytochemicals and structural disorder like with plant-mediated nanoparticle systems. The absorbance of the P sample decreases more rapidly with wavelength, reaching values as low as 0.65 a.u. at 1000 nm (about 65% of the original) and the T sample decreases more gradually to 1.05 a.u. (about 40% of the original). This difference in attenuation behaviour has been greatly ascribed to the improved light scattering and electronic localisation in non-uniform or defect-contaminated nanostructures, whereas thermally treated systems are more homogeneous and less scattered away. The smoother spectral profile of the thermally treated sample further suggests that the particles are more dispersed and that the electronic interaction between Fe and Cu is stronger indicating that the sample has been partially alloyed or the interfaces have been more strongly coupled, which has been shown to suppress discrete plasmonic features forming broadband absorption. The lack of discrete plasmonic characteristics has been observed in *Hibiscus rosa-sinensis*-based Fe nanoparticles, and *Camellia sinensis*-based Cu nanoparticles, in both cases electronic damping and structural heterogeneity suppressed plasmon resonance[18]. By contrast, the thermally treated Fe-Cu sample in the current study shows a smoother spectral decay, which is associated with less scattering losses and a higher electronic coupling, presumably due to a better alloying and structural homogeneity. Thus, it is evident that the spectral evolution of P to T is also an indication that thermal activation is a key factor in reducing optical losses, charge delocalization, and overall structural and electronic integrity of Fe-Cu bimetallic nanoparticles.

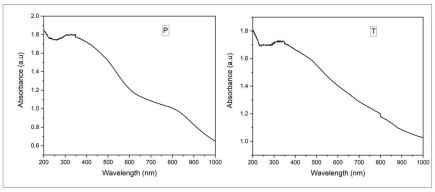

Figure 2 UV-visible spectroscopy analysis of as prepared and heat-treated Fe-Cu bimetallic nanoparticles

3.3 Raman spectroscopy analysis

The strong signal intensity and fluorescence interference in Raman spectroscopy in Fe-based nanostructures is frequently observed because of the residual phytochemicals in the green synthesis. Our experiment with the thermally treated sample yielded a poor Raman signal due to surface alteration and lower organic content. The Raman spectrum of the synthesized Fe–Cu bimetallic nanoparticles is shown in Figure 3. The spectrum shows typical vibrational bands of the iron oxide phases as well as the contribution of the bimetallic system. A major Raman band at the vicinity of 660-680 cm^{-1} is attributed to the A_1g symmetric stretching mode of FeO bonds in spinel-type iron oxide (Fe_3O_4) which validates the existence of magnetite-like structures. Other bands that emerge close to 300 cm^{-1} and 540 cm^{-1} are T_2g and Eg vibrational modes respectively that are also characteristic of Fe_3O_4. The existence of these bands shows that iron is mainly in the form of oxide in the synthesized nanoparticles. The peak broadening observed indicates some nanoscale crystallinity and potential lattice strain effects, which are typically linked to green-synthesized nanoparticles[19]. Moreover, a minor difference in the positions of the peaks relative to the values in literature could be explained by the interaction of Fe and Cu and distortion of the lattice, which proves that the incorporation of Cu affects the iron oxide structure. They display no prominent peaks that would imply a definite crystalline phase of Cu or CuO, indicating that copper is either well diffused or in an amorphous or low concentration state. This is common in bimetallic systems in which one of the metals is distributed at the interface and not crystallized. In general, Raman analysis has proved the presence of spinel-type iron oxide with potential Cu interaction, which is consistent with the findings of the XRD analysis and shows that the synthesis of Fe–Cu bimetallic nanoparticles had been successful.

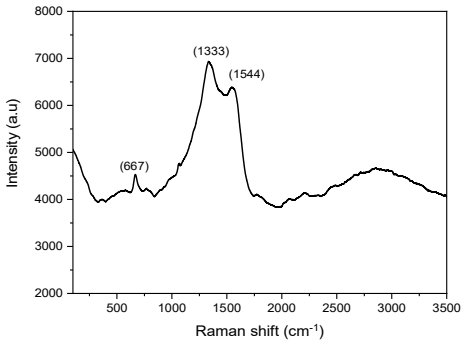

Figure 3 Raman analysis of as prepared and heat-treated Fe-Cu bimetallic nanoparticles

3.4 XRD analysis

Figure 4 shows the X-ray diffraction patterns of post-treated (P) and thermally treated (T) Fe–Cu bimetallic nanoparticles. The observed diffraction peaks of 2ɵ = approximately 30.2, 35.5º, 43.3º, 53.6º and 62.7º may be indexed to (2 2 0), (3 1 1), (4 0 0), (4 2 2) and (5 1 1) crystallographic planes respectively, and includes the contribution of metallic Cu phases. A sharp peak at 2ɵ of approximately 43.3º is also associated with the (1 1 1) face-centered cubic (fcc) Cu which shows the existence of Cu domains in the bimetallic system. The fact that these peaks coexist proves the existence of a heterostructure Fe-Cu nanocomposite, and not an alloyed phase. The minor changes in peak positions relative to standard JCPDS data indicate the lattice distortion due to interfacial interaction between Fe and Cu and some incorporation of the latter into an iron oxide lattice. The post-treated sample has wider and less sharp peaks, which shows smaller crystallites size, more strain in the lattice, and some amorphous nature of the sample because of the remaining phytochemicals in the plant extract. In contrast, the thermally treated sample shows sharper and more intense diffraction peaks, confirming enhanced crystallinity and improved phase segregation. The Scherrer equation was used to determine the average crystallite size (D), and the results obtained were about 23 nm and 42 nm, respectively, of P and T samples, respectively, which is indicative of a thermally induced grain growth. The growth of crystallites size is explained by better diffusion and recombination of atoms under thermal treatment. Also, the decrease in the broadening of the peaks indicates that there is a decrease in the micro strain and the density of defects. Thus, the XRD analysis reveals that the thermal treatment leads to the structural ordering, higher crystallinity, and stability of the Fe-Cu heterostructure, which is likely to have a substantial impact on the dielectric and electronic behaviour of the material.

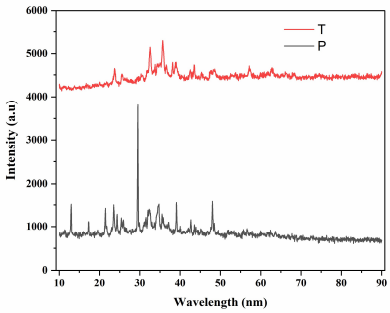

Figure 4 XRD analysis of as prepared and heat-treated Fe-Cu bimetallic nanoparticles

3.5 SEM analysis

The SEM micrographs (Figure 5(a–d)) clearly show that the post-treated (P), and thermally treated (T) Fe–Cu bimetallic nanoparticles. Figure 5(a-c) shows dense and highly agglomerated clusters which have undefined particle boundaries and rough surface texture in the post-treated sample. The particles are seen to be in the form of continuous networks and not discrete, which implies that there are strong interparticle interactions. This renders precise size measurement inaccurate; hence a rough distribution of nanoscale features can only be deduced, indicating the existence of small primary particles that are entrap inside larger aggregates[20]. The roughness and the non-uniform contrast that is observed are additional indications of unfinished growth and some form of residual phytochemical species that forms as weak stabilizing agents.

Conversely, the thermally treated sample (Figure 5(d-f)) is characterized by a comparatively better morphological definition, where the features of the particles can be partially distinguished and there is a decreasing agglomeration relative to the post-treated system. Despite the fact that individual particles are still interrelated, the surface is relatively smoother and localized areas are hinting at the development of quasi-spherical domains[21]. The visible growth of the size of features and the enhancement of the structural coherence can be attributed to the thermally driven grain growth seen in XRD analysis. Nonetheless, the measured dimensions are to be considered as aggregate or cluster size, as opposed to actual primary particle size, because of constant aggregation and an irregular geometry. The morphological changes of the highly disordered, rough agglomerates to relatively smooth and structured structures after thermal treatment suggest increased atomic diffusion, some part of the surface-bound organic residues, and enhanced interfacial contact between Fe and Cu elements. This behavior is characteristic of plant-mediated bimetallic systems, in which thermal activation allows bends to rearrange and surface

defects to be eliminated[22]. Altogether, SEM analysis does prove the thermal treatment to enhance morphological uniformity and structural integrity.

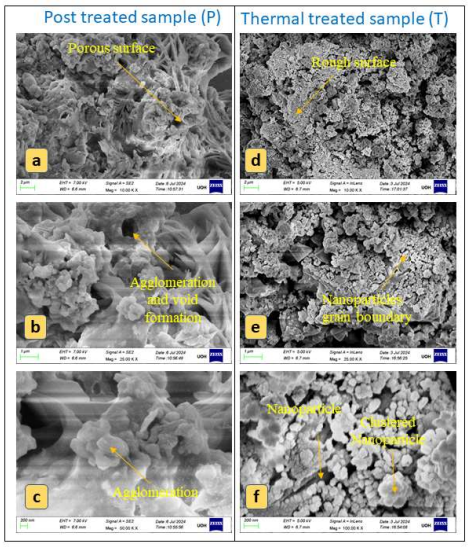

Figure 5 SEM analysis of as prepared and heat-treated Fe-Cu bimetallic nanoparticles

3.5 Dielectric property analysis

Figure 6(a&f) shows the frequency-dependent dielectric and impedance characteristics of the synthesized Fe-Cu bi-metallic nanoparticles. The dielectric constant (ε) and dielectric loss (ε'') in Figure 6(a) and Figure 6(b) have a high-frequency dispersion at lower frequencies and a gradual decrease and level-off at higher frequencies. This conduct is typical of Maxwell Wagner interfacial polarization, where the charge carriers concentrate at the grain boundaries and the interfaces when the frequency is low leading to large values of permittivity. With higher frequency, the dipolar entities cannot keep pace with the fast-varying electric field and both ε and ε'' get smaller. The trend in both parameters is similar, and this implies that mechanisms of polarization dominate the low-frequency domain and decrease with frequency. This behaviour is supported by the impedance components. The real component of impedance (Z), as shown in Figure 6(e) reduces with frequency, which implies that charge carrier mobility and resistance are reduced at higher frequencies. This trend implies that in the lower frequencies, space charge effects are dominant, and at higher frequencies bulk conduction takes over. The imaginary impedance (Z″) as in Figure 6(c) has a dispersion that reaches a peak and then decreases showing that there is a relaxation process that is related to charge carrier hopping and localized polarization. The non-Debye type relaxation is suggested by the shift and broad nature of the curve, and is usually seen in the heterogeneous nanostructured systems. The complicated impedance dependence as shown in Figure 6(d) (Z vs Z). The fact that it is not a perfect semicircle suggests that there is distributed relaxation time and structural inhomogeneity in the system. This further indicates that there exist interfacial polarization and non-uniform charge transport pathways in the material[23]. The behaviour of electric modulus (Figure 6(f)) gives further understanding of relaxation dynamics. The modulus rises with frequency, which means the elimination of the effects of polarization of electrodes and emphasizes bulk relaxation. The lack of a clear peak indicates that the relaxation is diffuse and distributed instead of just a well-defined process, which is in line with the complexity of the microstructure of bimetallic nanoparticles[24]. Thus, the analysis of the dielectric and impedance characteristics of the Fe-Cu nanostructures shows that interfacial polarization, hopping conduction, and non-Debye relaxation control the electrical behaviour of the Fe-Cu nanostructures. The measured reduction in impedance and dielectric values as frequency increases and dispersion of modulus, confirms enhanced charge transport and frequency-dependent electrical response, and these materials are useful in dielectric and electronic applications.

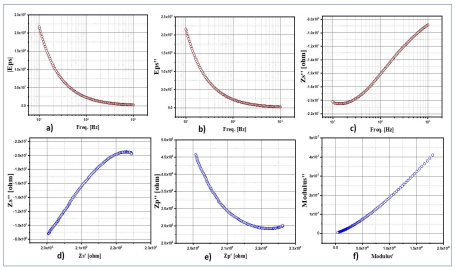

Figure 6: Figure the frequency-dependent dielectric and impedance characteristics of the synthesized Fe-Cu bi-metallic nanoparticles

Conclusion

Caralluma attenuata root extract was used as a reducing and stabilizing agent to successfully produce Fe–Cu bimetallic nanostructures through a green route. The structural analysis proved that there is a heterostructure system of spinel iron oxide with dispersed Cu domains. The crystallinity was improved on thermal treated sample which was resulted in XRD analysis. The presence of phytochemicals in the formation of nanoparticles was confirmed by FTIR, and the optical homogeneity was improved by thermal treatment according to UV-vis analysis. SEM analysis shows that heat treated samples show good interfacial surface properties and reduced agglomeration in nanoparticles system. Dielectric (50 Hz-5 MHz) measurements showed frequency dependent behaviour which was due to Maxwell Wagner interfaces polarization and non-Debye relaxation with charge transport increasing with frequency. Thus, the research shows that green synthesis followed by thermal processing can produce stable Fe-Cu nanostructures that have structural and electrical characteristics, which can be used in catalytic and dielectric applications.

Acknowledgement
We expresses sincere gratitude to the supporting institutions and laboratories that facilitated this research work.

Conflict of Interest
We declare no conflict of interest.

Data Availability
The corresponding author may be contacted with any legitimate request to get the data supporting this study's findings.

References

[1] T. S. Merjan and Z. T. A. Ali, "Green synthesis of bimetallic and trimetallic nanoparticles on glass granules for lead removal," *Desalination Water Treat.*, vol. 322, p. 101082, 2025, doi: https://doi.org/10.1016/j.dwt.2025.101082.

[2] A. Seid-Mohammadi, G. Asgari, A. Rahmani, T. Madrakian, and A. Karami, "Synthesis and application of iron/copper bimetallic nanoparticles doped natural zeolite composite coupled with ultrasound for removal of arsenic(III) from aqueous solutions," *Desalination Water Treat.*, vol. 162, p. 402, 2019, doi: https://doi.org/10.5004/dwt.2019.24786.

[3] Y. Su *et al.*, "Facile and green synthesis of Ag/Cu bimetallic nanoparticles using waste banana peel extract for effective corrosion inhibition of mixed sulfate-reducing bacteria," *J. Environ. Manage.*, vol. 373, p. 123713, 2025, doi: https://doi.org/10.1016/j.jenvman.2024.123713.

[4] Y. Wang, H. Zhao, and G. Zhao, "Iron-copper bimetallic nanoparticles embedded within ordered mesoporous carbon as effective and stable heterogeneous Fenton catalyst for the degradation of organic contaminants," *Appl. Catal. B*, vol. 164, pp. 396–406, 2015, doi: https://doi.org/10.1016/j.apcatb.2014.09.047.

[5] Y. Wu *et al.*, "Surface regulating of copper-iron nanoparticles bimetallic exsolution for enhanced performance and durability of double perovskite anode in solid oxide fuel cells," *Fuel*, vol. 353, p. 129140, 2023, doi: https://doi.org/10.1016/j.fuel.2023.129140.

[6] A. Selvaraj, K. Mukundamurthy, R. Rajmohan, and P. Tamizhdurai, "Simple one pot green synthesis of silver-palladium bimetallic nanoparticles: A fluorescent turn-off sensor for detection of lead ions in environmental water and its photocatalytic activity," *S. Afr. J. Chem. Eng.*, vol. 52, pp. 243–257, 2025, doi: https://doi.org/10.1016/j.sajce.2025.03.001.

[7] K. D. Vo *et al.*, "Iron-copper bimetallic nanoparticles dispersed within alginate-derived porous carbon: One-pot fabrication, characterization, and efficient peroxydisulfate activation for acid red 73 degradation," *Sustainable Chemistry for Climate Action*, vol. 8, p. 100179, 2026, doi: https://doi.org/10.1016/j.scca.2025.100179.

[8] P. Kansal, A. Shukla, and R. K. Shukla, "Valorization of seasonal waste Ficus rumphii leaves for green synthesis of mono and bimetallic nanoparticles: Characterization and their biological applications," *Sustainable Chemistry One World*, vol. 7, p. 100104, 2025, doi: https://doi.org/10.1016/j.scowo.2025.100104.

[9] L. Zhou, L. Yin, and Z. Chen, "Iron-palladium bimetallic nanoparticles embedded in metal organic frameworks nanocomposite adsorbents for arsenite and arsenate removal from groundwater," *Inorg. Chem. Commun.*, vol. 181, p. 115213, 2025, doi: https://doi.org/10.1016/j.inoche.2025.115213.

[10] A. Bendehhou *et al.*, "Green synthesis, characterization, and electrochemical nitrate sensing performance on three-dimensional iron–copper mixed oxide nanoparticles derived from coriander extract," *J. Environ. Chem. Eng.*, vol. 14, no. 3, p. 122398, 2026, doi: https://doi.org/10.1016/j.jece.2026.122398.

[11] C. P. Devatha, A. K. Thalla, and S. Y. Katte, "Green synthesis of iron nanoparticles using different leaf extracts for treatment of domestic waste water," *J. Clean. Prod.*, vol. 139, pp. 1425–1435, 2016, doi: https://doi.org/10.1016/j.jclepro.2016.09.019.

[12] P. Manickam-Periyaraman *et al.*, "Bimetallic iron-copper oxide nanoparticles supported on nanometric diamond as efficient and stable sunlight-assisted Fenton photocatalyst," *Chemical Engineering Journal*, vol. 393, p. 124770, 2020, doi: https://doi.org/10.1016/j.cej.2020.124770.

[13] A. Azeem *et al.*, "Green synthesis and eco-biological evaluation of Ag/Fe bimetallic nanoparticles using Vallaris solanacea leaf extract targeting insecticide resistance," *Particuology*, vol. 97, pp. 80–98, 2025, doi:

https://doi.org/10.1016/j.partic.2024.12.003.

[14] V. Bachhar, V. Joshi, A. Bhatia, T. Rom, M. Duseja, and R. K. Shukla, "Green synthesis of AgFe bimetallic nanoparticles from Calyptocarpus vialis plant extract for enhanced catalytic reduction of 4-NP, antioxidant and antibacterial activities," *J. Environ. Chem. Eng.*, vol. 13, no. 3, p. 116829, 2025, doi: https://doi.org/10.1016/j.jece.2025.116829.

[15] A. Hamza, M. K. Chan, K. C. Ho, Y. J. King, and P. Subhramaniyun, "Integration of used water filters and immobilized bimetallic iron-copper nanoparticles for rubber wastewater treatment," *Sep. Purif. Technol.*, vol. 379, p. 135039, 2025, doi: https://doi.org/10.1016/j.seppur.2025.135039.

[16] N. P. Sunesh *et al.*, "Detailed analysis and characterisation of microcrystalline cellulose derived from Ocimum tenuiflorum leaves," *Biomass Convers. Biorefin.*, vol. 15, no. 14, pp. 21573–21588, Jul. 2025, doi: 10.1007/s13399-025-06645-y.

[17] P. Meghwar *et al.*, "Synergistic use of Punica granatum peel and Moringa oleifera leaf to develop a functional and sustainable decoction," *J. Agric. Food Res.*, vol. 15, p. 101014, 2024, doi: https://doi.org/10.1016/j.jafr.2024.101014.

[18] R. Tamang, A. K. Mehata, V. Singh, M. S. Muthu, and B. Koch, "'Sustainable synthesis of Camellia sinensis-mediated silver nanoparticles (CsAgNP) and their anticancer mechanisms in breast cancer cells,'" *Biomaterials Advances*, vol. 166, p. 214072, 2025, doi: https://doi.org/10.1016/j.bioadv.2024.214072.

[19] Y. Lin, X. Jin, G. Owens, and Z. Chen, "Simultaneous removal of mixed contaminants triclosan and copper by green synthesized bimetallic iron/nickel nanoparticles," *Science of The Total Environment*, vol. 695, p. 133878, 2019, doi: https://doi.org/10.1016/j.scitotenv.2019.133878.

[20] B. Patel *et al.*, "Green synthesis of Ag–Fe bimetallic nanoparticles using fungal filtrates: unlocking multifunctional medical and environmental applications," *RSC Adv.*, vol. 15, no. 3, pp. 1565–1575, 2025, doi: 10.1039/D4RA07541B.

[21] K. Seethalakshmi, N. Mustapha, M. Gurumoorthy, K. Jayachitra, A. Muthuvel, and M. Hjiri, "Nanostructural design of ZnSe bimetallic nanoparticles via green synthesis for optimized photocatalytic and antibacterial applications," *Materials Science and Engineering: B*, vol. 329, p. 119430, 2026, doi: https://doi.org/10.1016/j.mseb.2026.119430.

[22] A. A. Akinsiku *et al.*, "Modeling and Synthesis of Ag and Ag/Ni Allied Bimetallic Nanoparticles by Green Method: Optical and Biological Properties," *Int. J. Biomater.*, vol. 2018, pp. 1–17, 2018, doi: 10.1155/2018/9658080.

[23] S. M. Al-Moayid, H. Algarni, H. E. Ali, and Y. Khairy, "Synthesis of reduced graphene oxide decorated with cuprite nanoparticles for energy-storage devices: Dielectric properties and electrical conductivity," *Physica B Condens. Matter*, vol. 714, p. 417490, 2025, doi: https://doi.org/10.1016/j.physb.2025.417490.

[24] A. Lakshmanan *et al.*, "Investigations on structural, optical, dielectric, electronic polarizability, Z-scan and antibacterial properties of Ni/Zn/Fe2O4 nanoparticles fabricated by microwave-assisted combustion method," *J. Photochem. Photobiol. A Chem.*, vol. 402, p. 112794, 2020, doi: https://doi.org/10.1016/j.jphotochem.2020.112794.